



Tartaruga, I., Cooper, J., Lowenberg, M. H., Sartor, P. N., Coggon, S., & Lemmens, Y. (2016). Prediction and uncertainty propagation of correlated time-varying quantities using surrogate models. *CEAS Aeronautical Journal*, 7(1), 29-42. DOI: 10.1007/s13272-015-0172-1

Peer reviewed version

License (if available):
Unspecified

Link to published version (if available):
[10.1007/s13272-015-0172-1](https://doi.org/10.1007/s13272-015-0172-1)

[Link to publication record in Explore Bristol Research](#)
PDF-document

University of Bristol - Explore Bristol Research

General rights

This document is made available in accordance with publisher policies. Please cite only the published version using the reference above. Full terms of use are available:
<http://www.bristol.ac.uk/pure/about/ebr-terms.html>

Prediction and Uncertainty Propagation of Correlated Time-Varying Quantities using Surrogate Models

I. Tartaruga[§], J.E. Cooper[§], M.H. Lowenberg[§], P. Sartor[§], S. Coggon[#], Y. Lemmens⁺

[§]Dept of Aerospace Engineering, University of Bristol, UK

[#]Airbus Operations Ltd, Filton, Bristol, UK

⁺Siemens, 3001 Leuven, Belgium

Corresponding author:

Irene Tartaruga, Dept of Aerospace Engineering, University Of Bristol, Queens Building, University Walk, Bristol, BS8 1TR, UK. E-mail: irene.tartaruga@bristol.ac.uk,

Abstract: The identification of correlated quantities is of particular interest in several fields of engineering and physics, for example in the development of reliable structural designs. When ‘time-varying’ quantities are analyzed, pairs of correlated Interesting Quantities (IQs) e.g. bending moments, torques etc., can be displayed by plotting them against each other, and the critical conditions determined by the extreme values of the envelope (convex hull). In this paper, a reduced order singular value based modelling technique is developed that enables a fast computation of the correlated loads envelopes for systems where the effect of variation of design parameters needs to be considered. The approach is extended to efficiently quantify the effects of uncertainty in the system parameters. The effectiveness of the method is demonstrated by consideration of the gust loads occurring from the aeroelastic numerical model of a civil jet airliner.

Keywords Correlated Loads, Prediction, Uncertainty Quantification, Surrogate Models, Singular Value Decomposition, Kriging surrogates.

1 Introduction

The correlation of quantities is of importance in many different fields, such as physics, engineering and biology. Indeed, critical phenomena often occur at specific correlated values of physical quantities, for instance the 2D or 3D stresses relating to combined loading cases. It is of great interest in aircraft design to identify which are the critical loading events (e.g. gusts, manoeuvres, landing loads, etc.), at what design configuration and environmental conditions they occur, and where on the aircraft structure they have the greatest effect. A typical aircraft loads design process [1] involves monitoring many (1000s) of Interesting Quantities (IQs) (e.g. bending moments, torques, displacements, etc.) for a wide range (100,000s) of different load cases that the aircraft is likely to experience in-flight and on the ground. Each ‘loads loop’ simulates the response of a numerical aeroelastic aircraft model to these loads and determines the critical cases; these results are then fed into the structural design. Such a process is extremely time consuming.

It is usual to determine the extreme loads cases for 1D (single IQs) and 2D (correlated IQs) events. In the latter case, pairs of IQ response time histories are plotted against each other for a range of different load cases. The extreme vertices of the envelope encompassing these plots, determined using a convex hull¹, are often called ‘potato’ plots and determine the critical load cases that are then used to perform stress calculations. Figure 1 shows a typical response of a wing root bending moment for an aircraft subjected to a family of different length ‘1 – cosine’ (1MC) gusts [1] and it can be seen how the critical case depends upon the gust length L_g . Figure 2 shows the correlated plot for wing root bending moment and torque, again for different length 1MC gusts; the outer bounds of the convex hull fitted around the correlated time histories give rise to the familiar ‘potato’ plot.

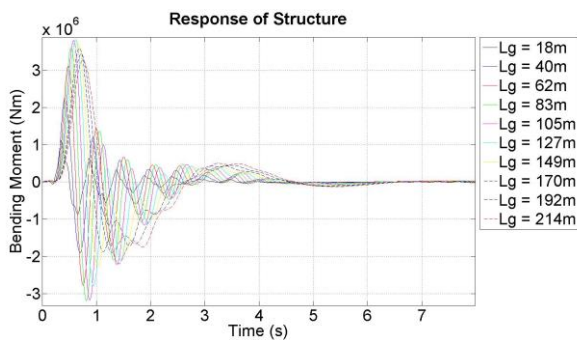


Fig. 1 IQ Time Histories for Different Gust Lengths

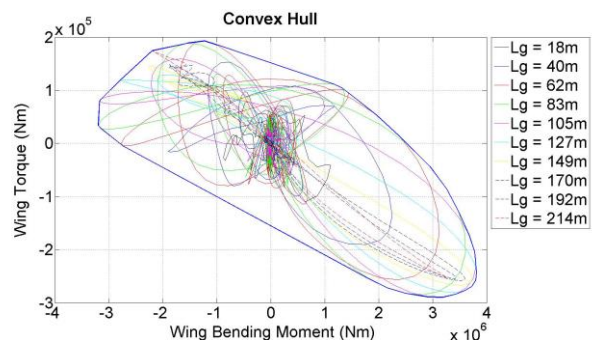


Fig. 2 2D Correlated Loads for Different Gust Lengths

¹ In this work, the Convex Hull envelope was determined using the MATLAB[®] function ‘convhull’.

Previous work in the FFAST FP7 project [2 - 5] has investigated the use of several surrogate models (also known as meta-models) and optimization methods for fast and efficient prediction of the worst case gust loads for each IQ of a civil jet airliner model. It was shown that considerable savings in computational time can be made without sacrificing accuracy. However, the IQs were dealt with independently and only a very preliminary investigation relating to the uncertainty quantification was undertaken [5] using a simple 2 degree of freedom (DOF) aeroelastic model and exploiting Polynomial Chaos Expansion (PCE) [6, 7, 8]. The PCE technique is one of several methods to quantify the uncertainty of some response quantity for which a statistical description of the inputs is known, and it is often applied to aleatory uncertainties in the aeronautical field. For example, uncertainties in the properties of composite structures [9 - 11] and in the stiffness of the structure [6, 12] have been studied to understand their effect on the flutter velocity [4, 9-11, 13-14].

In this work, a new method employing the Singular Value Decomposition (SVD) is described that enables a reduced order model (ROM) of the individual IQ time histories for different loading cases and design parameter variation to be produced. It will be shown how this approach not only enables efficient prediction of the 1D worst cases using Kriging surrogate models but, as the correlated time histories for different IQs are maintained, it is also possible to determine the correlated load plots for reduced computation without losing accuracy. A further advantage of this technique is that it is possible to use both a probabilistic approach and interval analysis to propagate the effect of uncertainties in the design parameters on each individual IQ and also the “potato” plots.

The effectiveness of the developed method is demonstrated by considering the IQs (bending moments and torques) arising from loads due to families of 1MC gusts acting upon a wing / pylon / engine structure of a typical civil jet aircraft numerical model. The effects of changes in the structural parameters on the IQs are modelled using the ROM approach and the effects of the uncertainty are quantified.

2 Aircraft and Load Models

The method developed in this work was implemented upon a numerical aircraft model subjected to vertical gust loads.

2.1 Aircraft Model

The aircraft model used is a representative civil jet airliner, the FFAST model [4], whose nominal weights and main dimensions are reported in Table 1. The structural model of the aircraft was a beam-stick model with lumped masses. (Figure 3) and the aerodynamics modelled using the *Doublet-Lattice Method* (DLM) [15].

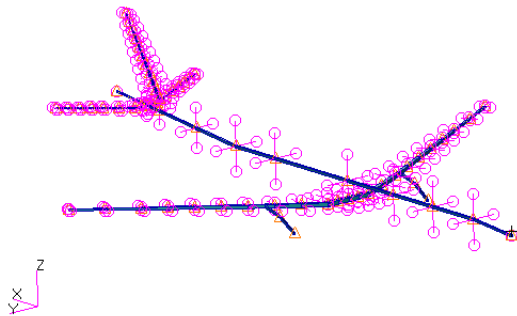


Fig. 3 Structural model of the aircraft

Weights		Dimension	
MTOW	231·10 ³ kg	Wing span	57.83 m
MLW	187·10 ³ kg	Mean chord	6.07 m
OEW	123·10 ³ kg		
MZFW	175·10 ³ kg	Other	
Max Payload	51.7·10 ³ kg	Cruise Speed	241.7m/s
Total fuel	110·10 ³ kg	Max operating altitude	12500 m
Mean Engine Weight	8694.3 kg		
Mean Wing Weight	3.2·10 ⁴ kg		

Table 1 Main weights and dimensions of the FFAST Model

2.2 Gust Model

The latest requirements for civil aircraft are found in the EASA Certification Specifications (CS-25) and Federal Aviation Regulations (FAR-25) [1,16]. In these requirements, two types of gust and turbulence are considered in order to represent the typical conditions that are met in flight:

- *Discrete gusts*, where the gust velocity is assumed to vary in a deterministic way. The most common shape is the so-called ‘1-cosine’ (1MC) profile.
- *Continuous turbulence*, where the gust velocity is considered to vary randomly.

In this work, 1MC gusts were considered (Figure 4) specified in the CS/FAR as [1]

$$U = \frac{U_{ds}}{2} \left[1 - \cos\left(\frac{\pi s}{H}\right) \right] \quad \text{for } 0 \leq s \leq 2H$$

where U is the gust velocity, U_{ds} is the design gust velocity, s is the distance penetrated into the gust and H is the gust gradient.

As the aim is to determine the critical response for each IQ, a sufficient number of gust gradient distances H in the range 9m to 107m must be investigated (gust length $L_g = 2 \times$ gust gradient).

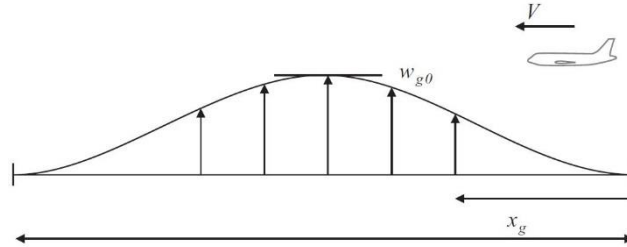


Fig. 4 Discrete ‘1-cosine’ gust [1]

Ten different gust gradients were considered as input cases across the following range of gust lengths: [18, 40, 62, 83, 105, 127, 149, 170, 192, 214] (all metres).

3 Method

The aim of this paper is to present a new method, described in Figure 5, to efficiently predict correlated quantities and corresponding convex hulls, in the presence of design parameter variations without sacrificing accuracy, and then to propagate the uncertainties. Here, variations in the structural parameters of the model civil jet airliner were considered; namely the mass, flexural and torsional stiffness of the wings, the mass of the engines and the stiffness of the pylons. Initially, the uncertainty in the mass of engine and the stiffness of pylon (in terms of Young Modulus) is considered, and then the complexity has been increased to include uncertainty in all the stated five parameters. The variations of the wing flexural (EI) and torsional (GJ) stiffness are in terms of inertia moments I and J, respectively. Regarding the mass of the wings, since the FFAST model presents structured mass and nonstructural mass (CONM2 and nstrM in Nastran), the variation of the mass of the wings has been obtained using the same scale factor m_f . Particular attention must be paid when the mass of the engine is changed; in fact, for such a component also the inertia moments have to be accordingly changed.

As well as determining the maximum and minimum response for each IQ [2 - 5, 19], it is also of interest to determine “correlated quantities”. For instance, the critical stresses / strains will be dependent upon a combination of Moment, Axial, Shear and Torque (MAST) loads. The correlated responses can be plotted against each other, determining the so-called “potato” plots. Figure 2 shows an example of correlated IQs in terms of wing loads: bending moment and torque. Once the configurations and environmental conditions to be analysed have been simulated, the outlying points of a convex hull are used to define the critical conditions at each station of a structure.

Note that both the IQ value and the time instants characterizing a critical case usually change as the parameters vary or different stations are considered; for instance, figure 6 shows the variation of the shape and area of the correlated loads plots along one wing. 10 stations have been considered from the root to the tip of the wing; note that variations in torque at the 7 outboard stations are negligible compared to the 3 inboard stations.

In order to speed up the process, the SVD is adopted to accomplish feature selection [17] in order to create surrogate models that are trained and validated using the Latin Hypercube Sampling (LHS) method [18].

The proposed method can be divided into three parts, which are discussed in detail as follows:

1. Application of the SVD
2. Surrogate Model Selection
3. Uncertainty Quantification

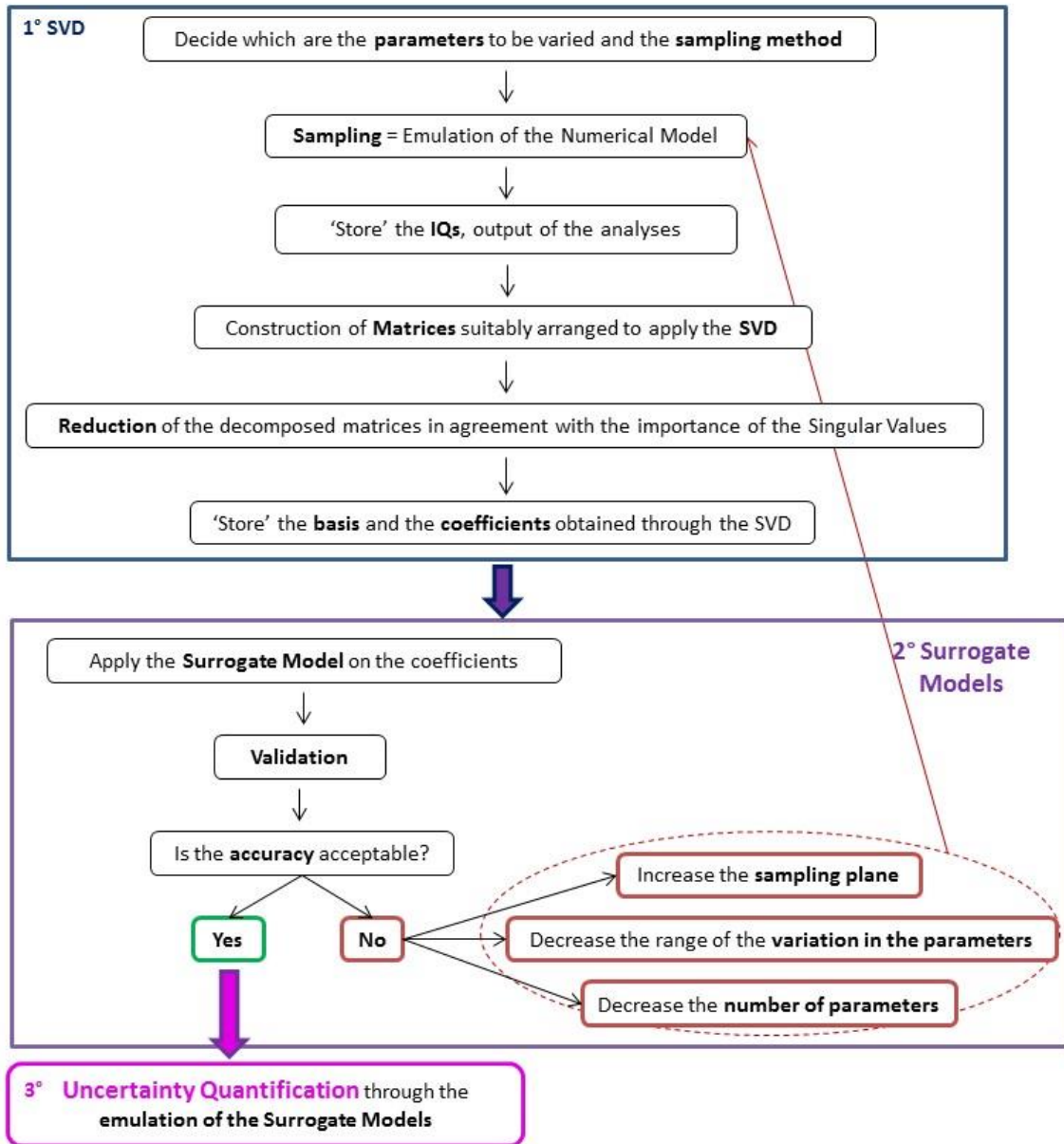


Fig. 5 Flow chart of the method

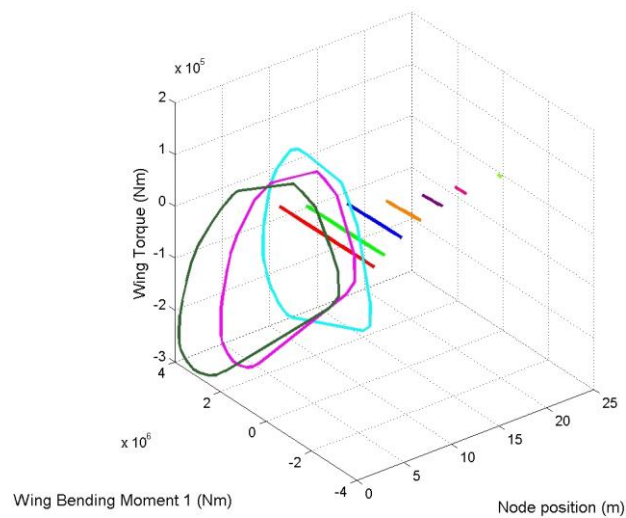


Fig. 6 Correlated loads envelope obtained at the wing root and its behaviour along the wing

3.1 Singular Value Decomposition

The Singular Value Decomposition (SVD) is a mathematical operation to decompose a rectangular matrix, used to analyze and simplify problems in several fields. In linear algebra it is commonly used to obtain ranks, kernels, norms and solution of simultaneous equations for over-determined systems. Moreover, it is very useful in data analysis, for instance noise removal, visualization and dimensionality reduction.

In the aeronautics field, the SVD has been used for over 30 years, applied to a range of different purposes including system identification and modal analysis. Recently, Sarkar et al. [22] have developed, demonstrated and tested a SVD-based method for symbolic design optimization problem reformulation, which has been applied to hydraulic cylinder design and aircraft concept sizing. Armstrong [23] used this technique to accomplish a down-selection procedure in terms of loads, identifying a suitable set of unit loads, and also to predict the response of a structure faster.

The SVD is defined as [20]: *for every matrix $\mathbf{A} \in \mathbb{R}^{m \times n}$ there exist two orthogonal matrixes $\mathbf{U} \in \mathbb{R}^{m \times m}$ and $\mathbf{V} \in \mathbb{R}^{n \times n}$ and a diagonal matrix $\mathbf{\Sigma} \in \mathbb{R}^{m \times n}$, whose diagonal contains the non-negative singular values $\lambda_1 \geq \lambda_2 \geq \dots \geq \lambda_{\min\{n,m\}} \geq 0$, such that \mathbf{A} can be decomposed as $\mathbf{A} = \mathbf{U}\mathbf{\Sigma}\mathbf{V}^T$.*

In order to reduce the dimension of a problem, \mathbf{A}_T , a truncated SVD can be considered. It is the matrix obtained considering only the columns of \mathbf{U} and \mathbf{V} (i.e. the *singular vectors*) related to the k highest singular values, i.e. \mathbf{U}_k and \mathbf{V}_k ; usually the non-zero singular values are chosen although this can be sometimes difficult to do in practice, and therefore the most significant terms are retained. Although several methods have been investigated (e.g. *Guttman-Kaiser criterion, Captured Energy, Cattell's Scree test*) a general approach that automatically identifies the correct rank for truncated SVD has not been yet identified, and this is mainly due to the inability on real data sets to determine where the cut-off needs to be made [21].

3.1.1 Application of Singular Value Decomposition for Feature Extraction

In this new method, the SVD is adopted for feature extraction. A major advantage of the developed method is that one can completely identify the cases (e.g. gust length), configuration and time instant which give the critical points of any part of the convex hull.

Initially, the parameters to be varied are decided upon (e.g. gust lengths, structural parameters, etc.), and two kinds of sampling points are determined using Latin Hypercube Sampling (LHS):

1. those that will be used to train the surrogate models (training points)
2. those that will be considered to validate the surrogate model (validation points)

Having saved all of the required time responses, a data matrix is constructed for each IQ of interest using the simulated gust response time histories as shown in Table 2. For example here, the Bending Moment and the Torque at 10 stations along each wing have been selected as IQs. The matrix, defined for each IQ, has as many rows as the number of parameter variations (e.g. engine mass, pylon stiffness) (D) and as many columns as the product of the number of time steps in each response (N), the number of configurations/ environmental conditions (e.g. case loads as gust lengths, altitudes) (M) and the number of stations of interest (S). Thus, the dimensions of each matrix are (D) x (NxMxS). The structure of the matrix is shown in Table 2.

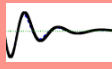
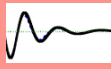
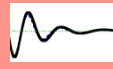
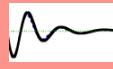
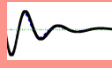
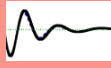
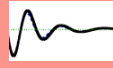
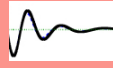
	Station 1			...	Station S		
	Case 1	...	Case M	...	Case 1	...	Case M
Training	Time (1:N)	...	Time (1:N)	...	Time (1:N)	...	Time (1:N)
1		...		...		...	
...
D		...		...		...	

Table 2 Matrix constructed for each IQ, before decomposition using the SVD

Each data matrix is decomposed using the truncated SVD and the product of the diagonal *singular value* matrix and the matrix containing the *right singular vectors*, i.e. $\Sigma_k V_k^T \in \mathbb{R}^{k \times n}$ is considered as a basis which is assumed not to change throughout the design space. Here the dimension of the basis is $(K) \times (N \times M \times S)$, where K is the number of singular values that are retained.

Then, surrogate models are developed for each column of the reduced matrix containing the *left singular vectors*, i.e. $U_k \in \mathbb{R}^{m \times k}$ modelling how they vary with respect to the design parameters. Figure 7 clarifies how the SVD is applied and then the surrogate models developed; in the 2D example shown the mass (M) of engine and pylon stiffness (E) are considered as design parameters.

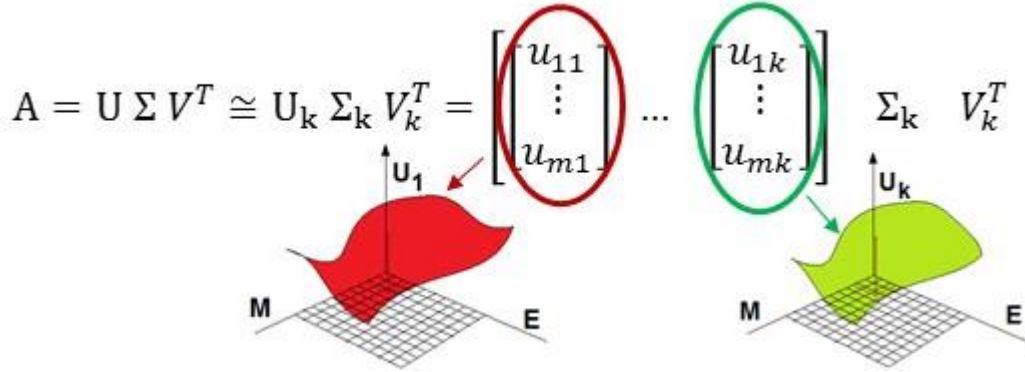


Fig. 7 Example of Surrogate Modelling Approach

Consequently, the time histories of each IQ at different stations, for different configurations / environmental conditions and for a specific i th sampling point can be simply identified by multiplying the respective row vector of coefficient $(U_k)_i$, determined by evaluating the surrogate models at the specific i th sampling point in the parameter space, by the fixed basis $\Sigma_k V_k^T$.

3.2 Surrogate Model Selection

After having identified these matrices, surrogate models of each of the K columns in the U matrix can be developed in order to enable both prediction and Uncertainty Quantification (UQ) of the correlated IQs. The use of surrogate models presents a key opportunity in all branches of physics and engineering to efficiently explore the design space, and also the effects of uncertainty, as they are able to simulate complex problems with the required accuracy without incurring too much computation.

Surrogate models [24] are developed using sampled data obtained by running simulations at particular training points in the region of interest. They have been applied in numerous fields, for instance: design space exploration, visualization, prototyping and sensitivity analysis [25], to deal with noisy or missing data, and also for data mining i.e. to understand which data/variables have the most impact [24]. Commonly used approaches include *Kriging* based methods, *Neural Network*, *Regression Tree* (Tree) and *Polynomial Radial Basis Functions* (Poly).

There are several different *Kriging* surrogate models; the differences between them are related to the particular form of the regression function that is used [24 -29]. The main approaches are:

- *Simple Kriging*, which assumes the regression function to be a known constant.
- *Ordinary Kriging* that considers a constant but unknown regression function ($f(\mathbf{x}) = \hat{\mu}$).
- *Blind Kriging*, which assumes the regression function to be a completely unknown function. This function is identified using a Bayesian variable selection technique.

The latter method, *Blind Kriging*, is preferable to the *Ordinary Kriging* approach, which suffers from:

1. Reduced performance in the presence of strong trends [30].
2. Lack of direct information about the effects of the factors (it is necessary to use a sensitivity analysis such as the functional analysis of the variance)
3. Lack of robustness in the presence of misspecification of the correlation parameters, which in turn are difficult to evaluate exactly.

For further details on how to construct the *Kriging predictors*, see [24, 25, 26, 28].

Polynomial Radial Basis Functions are regression models in which the selected basis is a polynomial [24] and *Neural Network* (NN) can be considered as a generalization of the Radial Basis Function; in fact the latter is a neural network with a single hidden Layer [17].

Moreover, there is a huge set of NN approaches that can be classified as follows:

- Feedforward Networks (MLP/Radial Basis Function)
- Recurrent Networks (Elman Networks) and
- Cellular Networks (Self-Organising Maps)

Finally, the *Regression Tree* method can be described as a series of logical if-then conditions (tree nodes) and is attractive due to its simplicity and lack of assumptions of linearity and/or monotonic link-functions between the output and input variables [31].

The aforementioned surrogate models have been compared in order to select the best for the present problem. Here, surrogate models are used to generate the row vector for any required parameter case. The row vector can be multiplied by the basis $\Sigma_k V_k^T$ to determine the time history of interest. Validation was performed by considering the Mean Absolute Percentage Error (MAPE) in terms of the maximum/minimum IQs. The MAPE was calculated by comparing the responses obtained using the full numerical model and those predicted using the SVD based method and is in general defined as

$$MAPE = \frac{1}{N} \sum_{k=1}^N \left| \frac{A_k - P_k}{A_k} \right|$$

where N is the number of validating points, A_k is the actual value and P_k is the predicted value.

Once the surrogate models are validated, if the accuracy is not acceptable for the analyzed problem, then possible solutions to improve the results are:

1. increase the number of test samples keeping the same variation in the parameters
2. decrease the range of the input parameters, or
3. decrease the number of parameters for which the prediction is required.

3.3 Uncertainty Quantification

UQ can be used to quantify the effects of uncertainty in the system parameters. The 1D case the variation of the maximum and minimum IQ values can be easily tracked [1], however the correlated time histories still need to be retained for each IQ. Using the reduced order surrogate model, it is possible to efficiently generate uncertainty bounds for the 1D time histories and the 2D correlated IQs plots using two approaches:

1. interval-confidence bounds, which considers the interval bounds of the IQs at each time instant;
2. quantile-confidence bounds, which considers the quantiles of the IQs at each time instant.

The interval bounds and the quantiles of the IQs, related to a specific time instant, are computed using the Kriging based surrogate model. Although the uncertainty quantiles of each element of the rows of U_k can easily be found, it is not possible to then obtain physically-meaningful quantiles for the time history simply by multiplying the fixed basis $\Sigma_k V_k^T$ by the determined quantile row vector of the coefficient U_k . Figure 7 shows typical trends for the 0.1, 0.5 and 0.9 quantiles for a typical IQ gust response time history. Note that the critical parameter case for each point on the quantile time histories is still maintained.

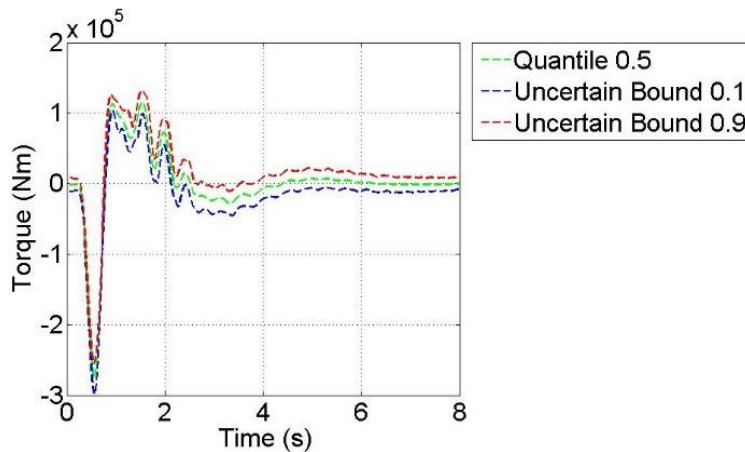


Fig. 7 Example of a time history (Torque) obtained for 0.1, 0.5 and 0.9 quantiles.

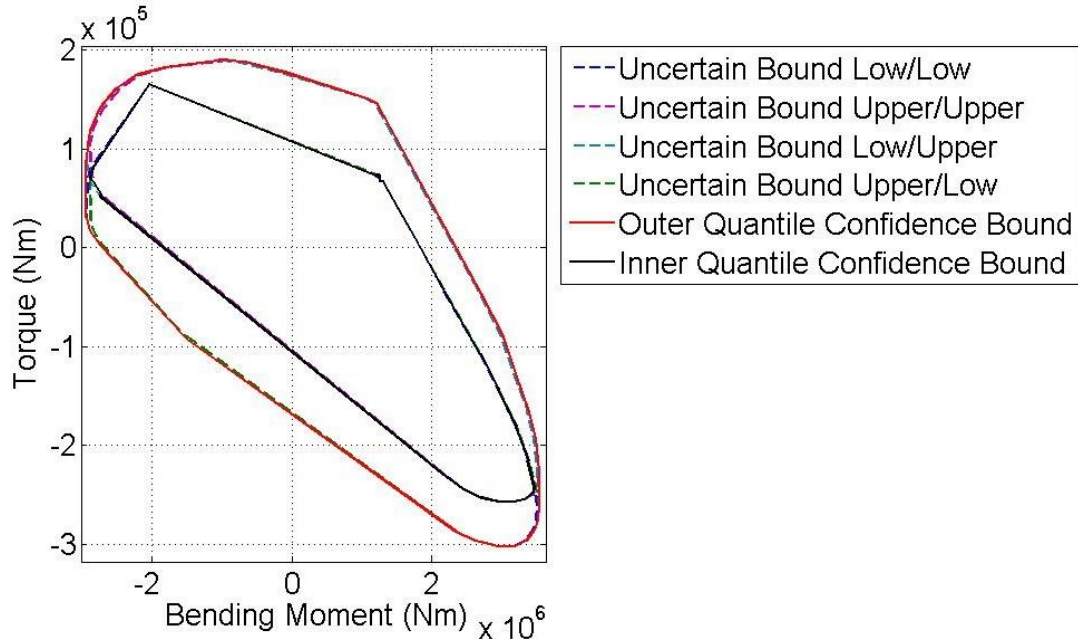


Fig. 8 Potato plot for two IQs and four different quantile combinations at the wing root.

Regarding the bounds for the convex hull of the correlated loads plots, the interval-confidence bounds can be obtained by only considering the envelope of all the computed convex hulls if the interval bounds of the time responses are considered. However, a more sophisticated approach needs to be used if the responses of interest are dealt with using the quantiles. In order to capture the greatest correlation between the time histories of the individual IQs, it is necessary to determine the convex hull of all possible combinations of the largest and smallest quantile bounds applied to each quantity, and then plot the inner and outer overall bounds. For the example shown in Figure 8, quantiles of $q = 0.1$ and $q = 0.9$ are taken and four convex hulls determined for all the possible combinations of correlated time histories i.e. [IQ1($q=0.1$) vs IQ2($q=0.1$), IQ1($q=0.1$) vs IQ2($q=0.9$), IQ1($q=0.9$) vs IQ2($q=0.1$), IQ1($q=0.9$) vs IQ2($q=0.9$)]. In this particular example, the convex hulls identified by points with the different Bending Moment quantiles are almost the same as the bending modes as they are less sensitive to different gust loads and variations in the structural parameters than the torsional modes. The overall outer curve is found using a convex hull applied to all four of the quantile time history combinations. The inner curve is identified in the same way, adopting both the ‘interval’ and the ‘quantile’ approach. Four plots are considered also for the interval approach; in particular, the quartet of points is identified by the lowest and highest value of each IQ i.e. [min(IQ1) vs min(IQ2), min(IQ1) vs max(IQ2), max(IQ1) vs min(IQ2), max(IQ1) vs max(IQ2)]. It should be noted that in this approach, the cases that lead to the critical correlated IQs are still maintained and can be identified.

4 Results and Discussion

Results using the methodologies discussed above were obtained for gust time history simulations for the wing/engine system. Initially, only variations in the mass of engine and the stiffness of pylon (in terms of Young Modulus) were considered, and then the complexity was increased to vary five parameters: the mass of the wings, wing flexural and torsional stiffness, and the engine mass and pylon stiffness. These cases are referred to as the 2D and 5D problems respectively. Table 3 shows the mean and the range adopted for the values of the structural parameters. The values assumed for the engine mass and the pylon Young modulus were selected according to the information provided in [6] and [32]. The mean of the inertia moments (I and J), the structured (CONM2) and unstructured mass (nstrM) of the considered 10 stations along the wing are shown in Table 4.

	Mean	Minimum	Maximum		Mean	Minimum	Maximum
Mass of Engine	8694.93 kg	-10%	+10%	m_f	-	-40%	+40%
Pylon Young Modulus	$69 \cdot 10^9$ Pa	-20%	+20%	I	-	-25%	+25%
				J	-	-25%	+25%

Table 3 Range of variation of the structural parameters

Element	I (m ⁴)	J (m ⁴)	nstrM (kg/m)
1	$2.12 \cdot 10^{-2}$	$7.78 \cdot 10^{-2}$	2122
2	$1.48 \cdot 10^{-2}$	$5.4 \cdot 10^{-2}$	1618
3	$9.97 \cdot 10^{-3}$	$3.63 \cdot 10^{-2}$	1258
4	$7.13 \cdot 10^{-3}$	$2.59 \cdot 10^{-2}$	1017
5	$5.19 \cdot 10^{-3}$	$1.88 \cdot 10^{-2}$	805.9
6	$3.38 \cdot 10^{-3}$	$1.22 \cdot 10^{-2}$	619.1
7	$1.8 \cdot 10^{-3}$	$6.52 \cdot 10^{-3}$	66.32
8	$5.21 \cdot 10^{-4}$	$1.92 \cdot 10^{-3}$	52.03
9	$3.45 \cdot 10^{-5}$	$1.32 \cdot 10^{-4}$	34.63

Station	CONM2 (kg)
1	666.1
2	881.8
3	665.8
4	515.5
5	408.3
6	314.8
7	233.5
8	183.5
9	131.2
10	56.08

Table 4 Nominal values of the changed structural parameters of each wing

4.1 Singular Value Decomposition Application

Both 2D and 5D sampling planes for the surrogate models training were considered in order to demonstrate how the accuracy increases in terms of the dimension of the sampling plane. Table 5 shows the number of samples that were considered and whether the z-score normalization was used; the adoption of a normalization approach and the number of Singular Values chosen depend upon the MAPEs discussed in Section 3.2. The aim was to capture those values that were significant for the prediction of the behaviour of the convex hull, even in the presence of uncertainty in the input parameters.

	2D		5D	
Training Points	100	240	600	1000
Validation Points	30	130	150	150
Singular Values:				
Bending Moment	1	1	30	30
Torque	22	30	50	50
Z-score Norm	YES	YES	NO	NO

Table 5 Adopted sampling plane and SVs

4.2 Surrogate Model: Training and Validation

All of the surrogate modelling methods discussed in Section 3.2 were implemented: *Neural Networks*, *Tree*, *Polynomial Radial Basis Functions* and *Kriging (Ordinary and Blind)*.

Figure 9 shows an example of a surrogate model of the first coefficient related to the torque responses obtained in the 2D problem with 100 training points. In Figures 10 and 11, the “potato” plots predicted adopting surrogate models, trained with 100 and 600 points respectively, are compared to the plot obtained from the numerical model (labelled with ‘No Reduction’). For the 5D problems, only the four surrogate models that showed the best results for the 2D problem were considered and the results are slightly less accurate, as it will be presented later in Table 7 and 8.

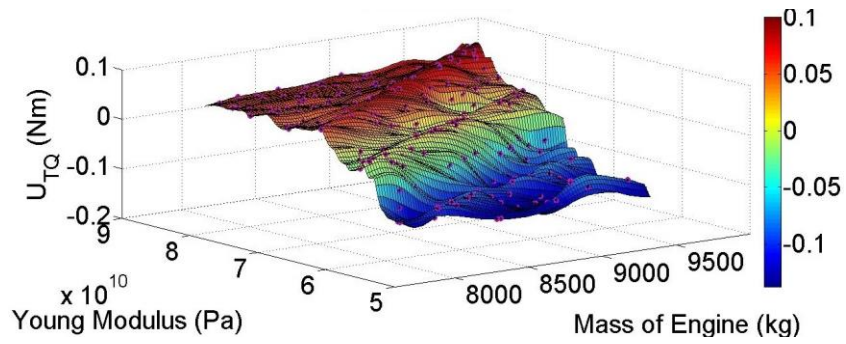


Fig. 9 Example of a Surrogate Model obtained in the 2D problem using the *Blind Kriging method* for the first coefficient related to the torque at the wing root.

After training, the surrogate models were validated for the deterministic responses exploiting the MAPE metrics, which were determined comparing the maximum/minimum IQs obtained using the numerical model and the SVD based method at the validation points (subsection 3.2). The results showed that the most accurate prediction compared to the “no reduction” case for the correlated loads envelope was obtained using the Blind Kriging method which always provides the smallest MAPEs.

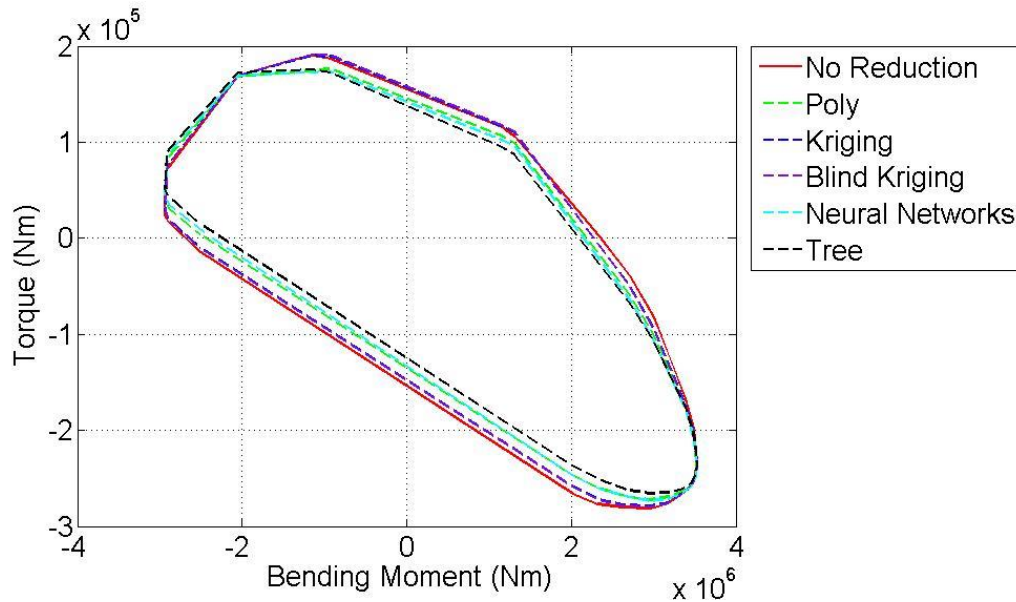


Fig. 10 Validation in terms of correlated load plots for the 2D problem at the wing root.

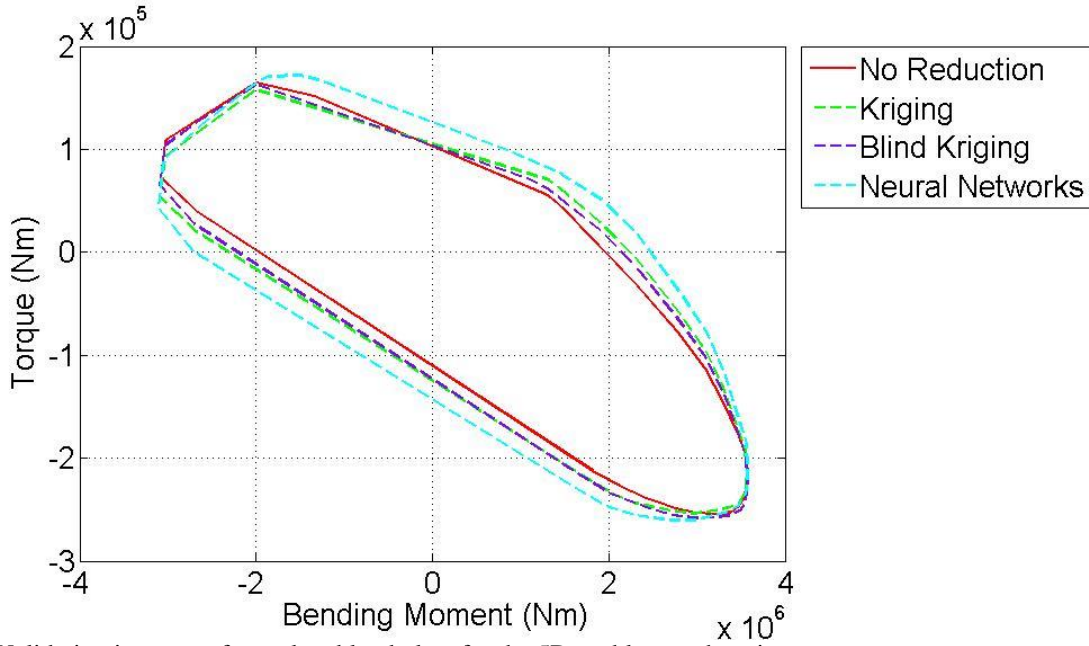


Fig. 11 Validation in terms of correlated load plots for the 5D problem at the wing root.

For the sake of clarity, Figure 12 shows in green and in red the 100 training sampling points and the 30 validating sampling points considered to train and validate the surrogate models obtained for the 2D problem, respectively. Table 6 summarizes the results obtained considering such sampling points. It shows the number of times in which each of the considered surrogate models is more accurate when compared to the others adopting the MAPE as the error metric. Tables 7 and 8 show the MAPEs obtained adopting the Blind Kriging surrogate models for all the stations for the 2D and 5D problems, respectively.

Surrogate Models	Kriging	Blind Kriging	Poly	Neural Network	Tree
Number	65	87	51	56	41

Table 6 Number of times a surrogate model is more accurate when compared to the others adopting the MAPE as the error metric and considering 30 validating points and all the 10 stations along the wing.

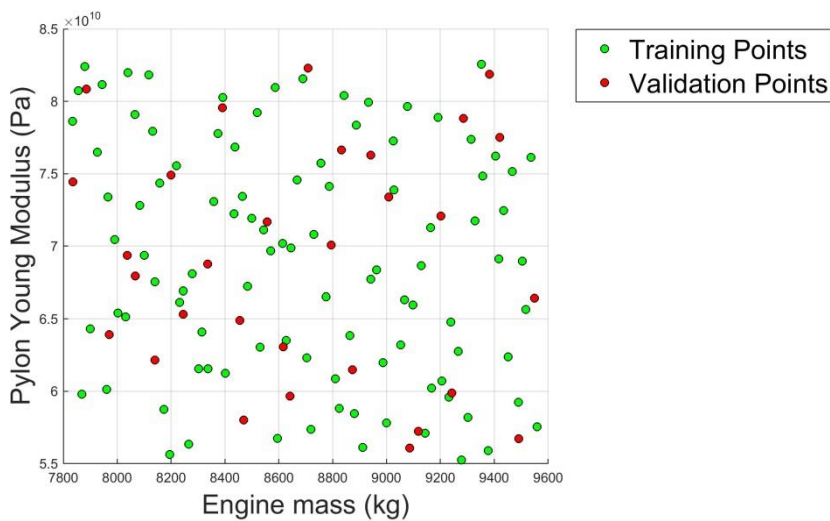


Fig. 12 Sampling plane in terms of the pylon Young modulus and engine mass.

Station:	1	2	3	4	5	6	7	8	9	10
	Maximum Bending Moment									
	<i>Training Points</i>									
100	0.09	0.06	0.26	0.21	0.21	0.21	0.22	0.24	0.46	0.61
240	0.08	0.06	0.23	0.22	0.22	0.21	0.22	0.25	0.44	0.57
	Minimum Bending Moment									
100	0.33	0.25	0.35	0.40	0.41	0.45	0.54	0.67	0.86	1.07
240	0.39	0.26	0.35	0.39	0.40	0.44	0.54	0.67	0.88	1.10
	Maximum Torque									
100	2.20	2.55	8.28	1.36	1.09	0.86	0.62	0.59	0.73	2.03
240	3.55	3.79	6.96	1.17	0.93	0.70	0.47	0.44	0.61	1.90
	Minimum Torque									
100	2.28	2.45	5.89	0.86	0.77	0.63	0.37	0.35	0.53	2.52
240	2.30	2.42	4.90	0.99	0.88	0.70	0.44	0.41	0.57	2.96

Table 7 Mean Absolute Percentage Error (%) Station by Station for the **2D SVD** based approach.

Station:	1	2	3	4	5	6	7	8	9	10
	Maximum Bending Moment									
600	0.16	0.14	0.26	0.25	0.28	0.29	0.32	0.40	0.59	0.98
1000	0.14	0.13	0.22	0.22	0.24	0.26	0.28	0.32	0.45	0.77
	Minimum Bending Moment									
600	0.37	0.26	0.47	0.38	0.38	0.41	0.46	0.54	0.61	1.02
1000	0.32	0.24	0.46	0.43	0.43	0.43	0.45	0.49	0.55	0.81
	Maximum Torque									
600	5.30	5.49	8.04	3.09	2.87	2.71	2.75	2.72	2.54	5.95
1000	5.29	5.62	7.19	2.99	2.82	2.63	2.85	2.77	2.44	5.38
	Minimum Torque									
600	2.64	2.72	5.38	2.46	2.38	2.18	1.89	1.93	2.58	6.26
1000	2.29	2.39	5.86	2.21	2.12	1.85	1.65	1.66	2.22	5.85

Table 8 Mean Absolute Percentage Error (%) Station by Station for the **5D SVD** based approach.

The key findings from the validation for both the 2D and 5D problems using the MAPEs show:

- best accuracy was achieved with the *Blind Kriging* surrogate model, in particular the evaluated MAPEs are always less than 8% for all the considered stations.
- the bending moment predictors were more accurate than the ones developed for the torque, which is due to the higher influence of the gust on the torsional modes.
- a slight improvement of the prediction if a higher number of training points was used.

4.3 Uncertainty Quantification

Results for the UQ are presented using the approaches discussed in subsection 3.3. The validation for the UQ has been accomplished by comparing with the results found using a Monte Carlo Simulation (MCS). The method for the *uncertainty propagation* presented in Section 3.3 was applied to the 2D and 5D problems, considering first the effects of uncertainty in the engine mass and stiffness of the pylon, and then in all the five parameters, namely the mass, flexural and torsional stiffness of the wings, the mass of the engines and the stiffness of the pylons. The adopted Blind Kriging surrogate models are those trained with 100 and 600 points for the 2D and 5D cases, respectively.

The uncertainties in terms of the engine mass and stiffness of pylon were modelled probabilistically, the PDFs have been assumed to be Gaussian and the main statistical quantities are summarized in Table 9. Since the range of variation adopted for these structural parameters, a sub-domain of the uncertain inputs is considered (Table 9). These subdomains capture 98.97% and 95.45% of the probability distribution for the mass of engine and stiffness of pylon, respectively.

The other structural parameters are considered to be primarily epistemic and their variation intervals are presented in Table 4.

	Mean μ	COV	σ
Mass of Engine	8694.93 kg	0.039	339.1 kg
Young Modulus of the Pylon	$69 \cdot 10^9$ Pa	0.1	$69 \cdot 10^8$ Pa

Table 9 Adopted statistical quantities

Figure 13 shows the bounds on the critical correlated load cases, which are expressed in terms of the lengths of gust (L_g), characterizing the interval confidence bounds of the convex hull and the “potato” plot for the 2D problem, which are detected using the SVD-based method together with the Blind Kriging Surrogate Models.

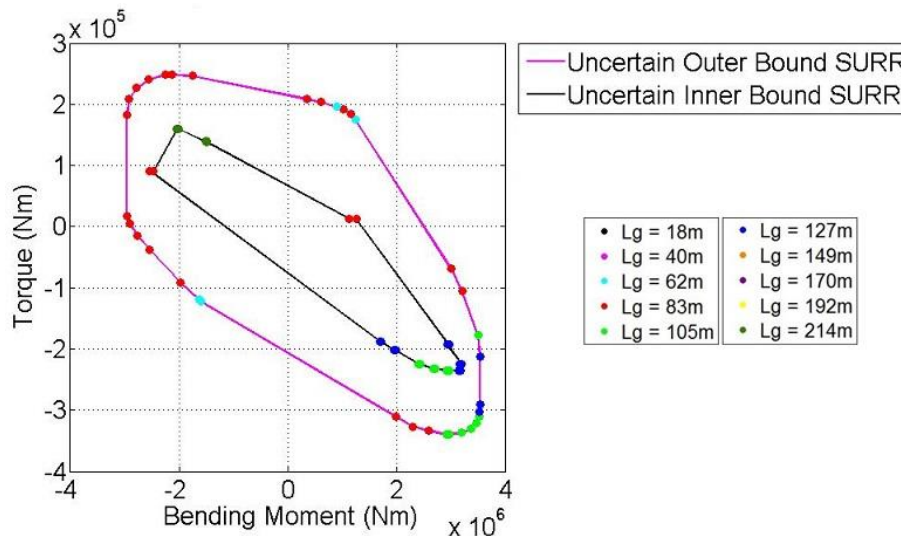


Fig. 13 Interval confidence bounds of the convex hull at the wing root, obtained applying the SVD-based method together with the Blind Kriging model (SURR) to the 2D problem. The coloured points on the bounds denote the critical cases.

Validation of UQ SVD-based methods

In order to validate the UQ, a Monte Carlo Simulation was conducted for the 2D and 5D problems and considered as actual. The numerical model was run 1200 times and 2400 times to validate the UQ performed for the 2D and 5D problems. The surrogate models were emulated 600, 1200 and 2400 times to check if differences in the results occurred. In all three cases, and for both the 2D and 5D problems, the estimated quantiles are practically the same and the results achieved the required accuracy. The results presented here were obtained by considering 1200 and 2400 emulations for the 2D problem and 5D problems, respectively. There was only a slight improvement when a higher number of emulations was adopted.

Figures 14 and 15 show a comparison of quantile - bounds of the convex hull and the mean (0.5 quantile) “potato” plot at three stations (at the wing root, just inboard of the engine and at the wing tip) for the 2D and 5D problems, respectively. In all the cases very good agreement was obtained; good results were also obtained when determining the interval confidence bounds.

The results from the *Blind Kriging* surrogate model have been compared with a MCS of the numerical model for a set of quantiles. Tables 10 and 12 shows the maximum of the absolute percentage errors of the maximum/minimum IQs, and for which quantile they are obtained, for all the stations along the wing for both the 2D and 5D problems. Finally, Tables 11 and 13 show the MAPE obtained for the maximum/minimum IQs considering the interval-confidence bounds and comparing the results with the ones obtained through MCS.

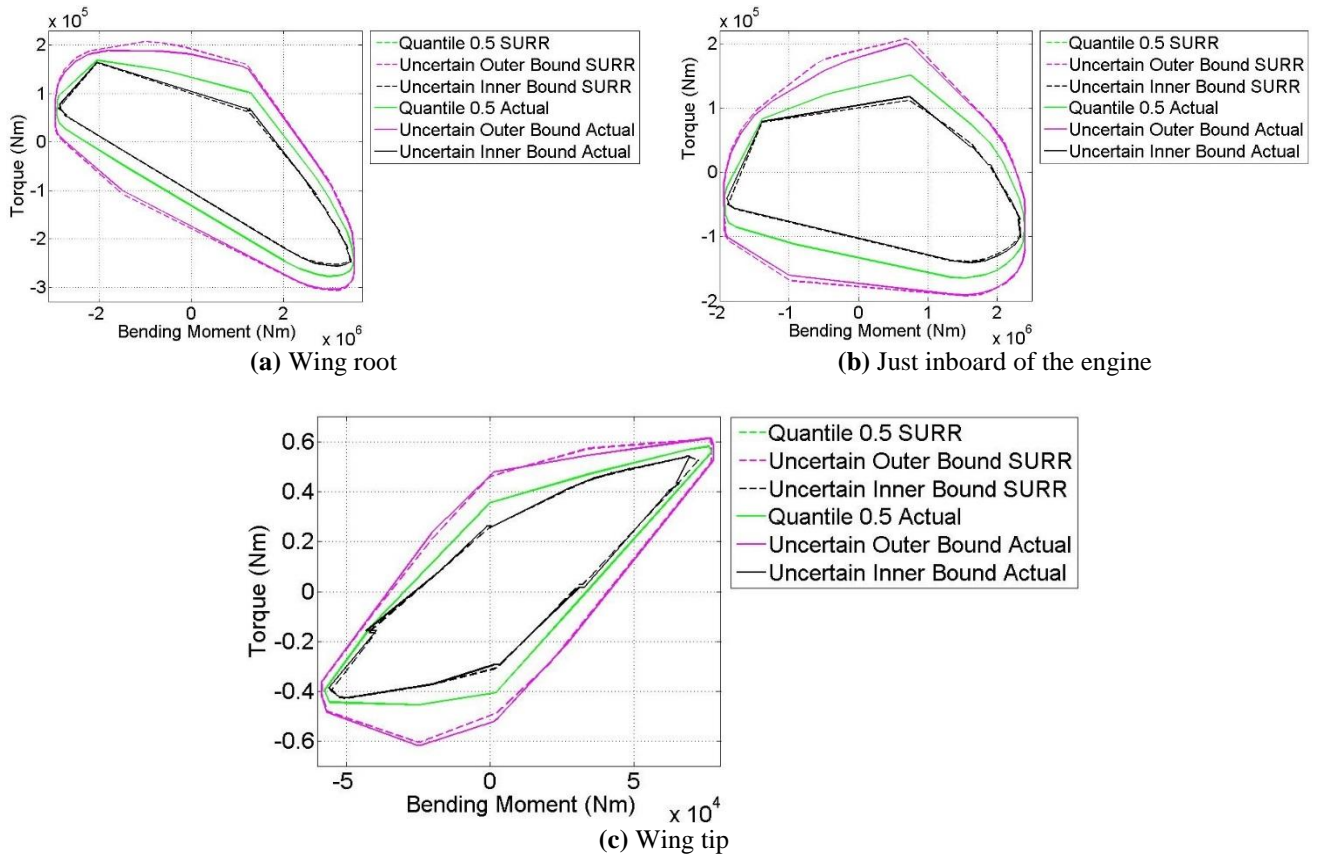


Fig. 14 Validation of the UQs for the 2D problem. Comparison of convex hulls obtained at three stations for a 10 1MC gust family using the emulation of the Blind Kriging surrogate model (SURR) and a MCS of the numerical model (Actual)

	Station									
	1	2	3	4	5	6	7	8	9	10
	Percentage Error Maximum Bending Moment									
Value	0.099%	0.046%	0.23%	0.29%	0.29%	0.3%	0.32%	0.36%	0.53%	0.86%
Quantile	0.3	0.3	0.7	0.9	0.9	0.9	0.9	0.9	0.1	0.1
	Percentage Error Minimum Bending Moment									
Value	0.34%	0.14%	0.45%	0.23%	0.24%	0.25%	0.28%	0.62%	0.64%	0.57%
Quantile	0.7	0.1	0.9	0.9	0.9	0.9	0.8	0.9	0.9	0.9
	Percentage Error Maximum Torque									
Value	6.8%	7.2%	6.9%	0.62%	0.48%	0.43%	0.22%	0.16%	0.37%	1.4%
Quantile	0.9	0.9	0.5	0.1	0.1	0.1	0.1	0.1	0.9	0.3
	Percentage Error Minimum Torque									
Value	1.2%	1.3%	1.9%	0.35%	0.37%	0.21%	0.13%	0.11%	0.17%	7.8%
Quantile	0.9	0.9	0.5	0.1	0.9	0.9	0.2	0.2	0.1	0.4

Table 10 Validation for the UQs of the 2D problem. Maximum of the absolute-percentage errors with respect to the MCS for the maximum/minimum IQs for each station and quantiles. The considered quantiles are from 0 to 1 with an increment of 0.1

	Station									
	1	2	3	4	5	6	7	8	9	10
	MAPE Maximum Bending Moment									
Value	0.14%	0.15%	0.21%	0.61%	0.63%	0.69%	0.72%	0.76%	1.18%	1.70%
	MAPE Minimum Bending Moment									
Value	0.09%	0.11%	0.96%	0.41%	0.43%	0.52%	0.98%	1.58%	1.56%	1.52%
	MAPE Maximum Torque									
Value	0.05%	0.05%	2.19%	0.16%	0.13%	0.25%	0.17%	0.15%	0.25%	2.17%
	MAPE Minimum Torque									
Value	1.38%	1.44%	0.60%	0.10%	0.15%	0.15%	0.11%	0.11%	0.16%	1.70%

Table 11 Validation for the UQs of the 2D problem considering the interval-confidence bounds. MAPE with respect to the MCS for the maximum/minimum IQs for each station.

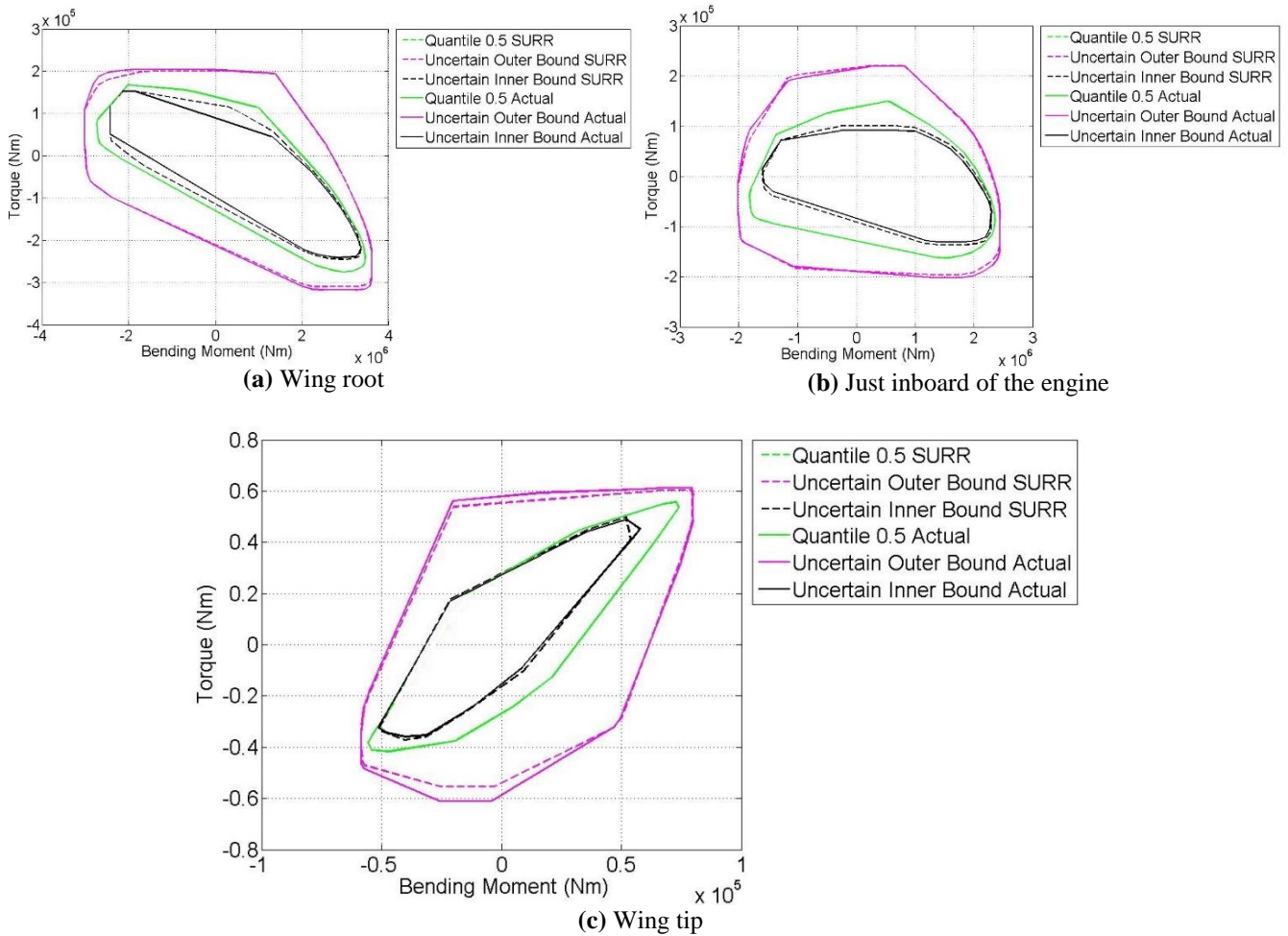


Fig. 15 Validation of the UQs for the 5D problem. Comparison of convex hulls obtained at three stations for a 10 1MC gust family using the emulation of the Blind Kriging surrogate model (SURR) and a MCS of the numerical model (Actual)

	Station									
	1	2	3	4	5	6	7	8	9	10
	MAPE Maximum Bending Moment									
Value	0.92%	0.73%	0.19%	0.30%	0.37%	0.04%	0.53%	0.76%	1.15%	2.58%
Quantile	0.1	0.1	0.1	0.2	0.1	0.2	0.1	0.1	0.1	0.1
	MAPE Minimum Bending Moment									
Value	1.10%	1.00%	0.80%	1.26%	0.95%	0.16%	0.06%	1.64%	1.92%	1.58%
Quantile	0.2	0.2	0.2	0.2	0.2	0.2	0.1	0.2	0.2	0.1
	MAPE Maximum Torque									
Value	0.99%	0.92%	13.08%	0.47%	1.01%	1.18%	0.68%	0.58%	2.23%	0.87%
Quantile	0.1	0.1	0.1	0.2	0.2	0.1	0.2	0.1	0.2	0.2
	MAPE Minimum Torque									
Value	3.45%	3.40%	4.05%	0.83%	1.87%	1.66%	1.20%	1.40%	1.92%	6.02%
Quantile	0.2	0.2	0.2	0.2	0.2	0.2	0.2	0.2	0.2	0.1

Table 12 Validation for the UQs of the 5D problem considering the quantile-confidence bounds. MAPE with respect to the MCS for the maximum/minimum IQs for each station and quantiles. The considered quantiles are from 0 to 1 with an increment of 0.1.

	Station									
	1	2	3	4	5	6	7	8	9	10
	MAPE Maximum Bending Moment									
Value	0.01%	0.06%	0.46%	0.34%	0.26%	0.36%	0.29%	0.50%	0.39%	2.73%
	MAPE Minimum Bending Moment									
Value	0.48%	0.49%	0.63%	0.74%	0.89%	0.66%	0.65%	1.62%	3.47%	1.36%
	MAPE Maximum Torque									
Value	4.47%	4.50%	7.39%	6.48%	6.22%	7.36%	8.39%	8.18%	7.30%	4.77%
	MAPE Minimum Torque									
Value	6.38%	6.62%	8.50%	5.90%	4.73%	3.63%	2.89%	3.05%	2.51%	10.61%

Table 13 Validation for the UQs of the 5D problem considering the interval-confidence bounds. MAPE with respect to the MCS for the maximum/minimum IQs for each station.

Even in the presence of errors, especially in terms of the torque as shown in table 12 and 13, it has been demonstrated that the required accuracy is excellent. Indeed, we have verified that adopting the developed method for the UQ, the required critical conditions for the aircraft are identified with very good accuracy: the *correlated loads* at different stations at the same critical case load and the *critical case loads* for all the desired stations are the same as those obtained adopting the MCS technique.

In addition, the developed method requires much less computation than MCS. For the 2D/5D problems analyzed, using a desktop PC, a MCS takes about two/five days to propagate the uncertainty, whereas the method presented in this paper requires two hours both to train all the surrogate models and propagate the uncertainty up to the convex hull. This is a reduction of approximately 95% in computation time.

5 Conclusions

A Singular Value Decomposition (SVD) based method for the efficient prediction and propagation of uncertainty of correlated ‘time-varying’ quantities has been presented and validated considering an aeroelastic model of a civil aircraft. For the prediction studies, the Blind Kriging surrogate model gave the most accurate results and good quality predictions were obtained considering variations for both two (2D) and five (5D) structural parameter variations. It has been shown that using the SVD, together with the Blind Kriging surrogate model, all the required information related to the behaviour of the correlated Interesting Quantities and the critical conditions can be captured using significantly reduced order models. Very good results were also achieved for the Uncertainty Quantification (UQ) both for the 2D and 5D problems,

using the SVD based approach, when compared to results from Monte Carlo Simulations with a significant reduction (approximately 95%) in computation. Future work will improve the implementation of the developed techniques, investigating the application to even higher order configurations and number of design parameters.

Acknowledgements

The research leading to these results has received funding from the European Community's Marie Curie Initial Training Network (ITN) on Aircraft Loads Prediction using Enhanced Simulation (ALPES) FP7-PEOPLE-ITN-GA-2013-607911. The partners in the ALPES ITN are the University of Bristol, Siemens and Airbus Operations Ltd.

References

- [1] J. R. Wright & J.E. Cooper, "Introduction to Aircraft Aeroelasticity and Loads", Wiley, 2007.
- [2] H.H. Khodaparast, G. Georgiou, J.E. Cooper, L. Travaglini, S. Ricci, S. Vio G.A., & P. Denner "Rapid Prediction of Worst Case Gust Loads", *J.Aeroelasticity and Structural Dynamics*. v2 n3 2012.
- [3] H.H. Khodaparast, Georgiou G., Cooper J.E., Travaglini L., Ricci S., Denner P. and Vio G.A.. "Efficient Worst Case '1 – Cosine' Gust Loads Prediction", IFASD 2011 Paris, France.
- [4] H.H. Khodaparast and J.E. Cooper. "Rapid Prediction of Worst Case Gust Loads Following Structural Modification" *AIAA Journal*, 2014 v52, n2 pp 242-254.
- [5] H.H. Khodaparast, J.E. Cooper, L. Cavagna, S. Ricci and L. Riccobene "Fast Prediction of Worst Case Gust Loads" *International Forum on Aeroelasticity and Structural Dynamics*, 2013.
- [6] S. K. Choi, R. V. Grandi, R. A. Canfield "Reliability-based Structural Design", Springer-Verlag London Limited 2010.
- [7] D. Xiu and G. E. Karniadakis, "The Wiener-Askey Polynomial Chaos for Stochastic Differential Equations", in *Society for Industrial and Applied Mathematics Journal on Scientific Computing (SIAM J.Sci)*, 2002, Vol.24, No. 2 pp. 619-644.
- [8] M. S. Eldred "Recent Advances in non-Intrusive Polynomial Chaos and Stochastic Collocation Methods for Uncertainty Analysis and Design", in *50th AIAA/ASME/ASCE/AHS/ASC Structures, Structural Dynamics, and Material Conference*, 4-7 May 2009, Palm Springs, California.
- [9] G. Georgiou, A. Manan & J.E. Cooper, "Modeling Composite Wing Aeroelastic Behaviour with Uncertain Damage Severity and Material Properties" *Mechanical Systems and Signal Processing*, Vol 32, October, 2012, pp. 32-43.
- [10] K.J. Badcock, H.H. Khodaparast, S. Timme and J.E. Mottershead, "Calculating the Influence of Structural Uncertainty on Aeroelastic Limit Cycle Response", *52nd AIAA/ASME/ASCE/AHS/ASC Structures, Structural Dynamics, and Materials Conference*, Denver, Colorado, 4-8 Apr. 2011.
- [11] C. Scarth, J.E. Cooper, P. M. Weaver, G H.C. Silva "Uncertainty Quantification of Aeroelastic Stability of Composite Plate Wings using Lamination Parameters" *Composite Structures* 2014 v116 pp 84-93.
- [12] S.K. Choi, R.V. Grandhi, R. A. Canfield & C. L. Pettit "Polynomial Chaos Expansion with Latin Hypercube Sampling for Estimating Response Variability", *AIAA Journal*, Vol. 42, No. 6, June 2004.
- [13] C.L. Pettit "Uncertainty Quantification in Aeroelasticity: Recent Results and Research Challenges", in *Journal of Aircraft*, Voll.41, No. 5, September-October 2004.
- [14] Q. Ouyang, X. Chen & J.E. Cooper, "Robust Aeroelastic Analysis and Optimization of Composite Wing Under μ -Analysis Framework", *J.Aircraft* Vol. 50, 2013, pp. 1299-1305.
- [15] E. Albano & W.P. Rodden, "A Doublet-Lattice Method for Calculating Lift Distributions on Oscillating Surfaces in Subsonic Flows" *AIAA J.* Vol. 7 n2 pp 279-285. 1969.
- [16] *Airworthiness Standards Part 25: Transport Category Airplanes, Subpart C, Structure, Flight Maneuver and Gust Conditions.* (§25.333 Flight maneuvering envelope, §25.341 Gust and turbulence loads), November 6, 2014.
- [17] K. Worden, W.J. Staszewski, J. J. Hensman, "Natural Computing for Mechanical Systems Research: A Tutorial Overview", *Mechanical Systems and Signal Processing*, Volume 25, Issue 1, January 2011, Pages 4-111.
- [18] J. C. Helton and F. J. Davis, "Sampling-Based Methods for Uncertainty and Sensitivity Analysis", SAND99-2240, Albuquerque, NM, Sandia National Laboratories, July 2000.
- [19] A. Manan & J.E. Cooper "Design of Composite Wings Including Uncertainties – A Probabilistic Approach", *J.Aircraft*. v46n2 2009 pp601-607.
- [20] G.H. Golub & C.F. Van Loan "Matrix Computations", 2nd ed. John Hopkins Press 1989.
- [21] R. Gemulla, P. Miettinen, "Data Mining and Matrices, Singular Value Decomposition", April 25, 2013. <http://resources.mpi-inf.mpg.de/d5/teaching/ss13/dmm/slides/03-svd-handout.pdf> downloaded in May 2014.
- [22] S. Sarkar, A. Dong, J. S. Gero, "Design Optimization Problem Reformulation using Singular Value Decomposition", *Journal of Mechanical Design*, 2009.
- [23] S. McGuinness, C.G. Armstrong, A. Murphy, J. Barron, M. Hockenull, "Improving Aircraft Stress-Loads Evaluation and Optimization Procedures", *2nd Aircraft Structural Design Conference*, London, United Kingdom, 2010.
- [24] A. Forrester, A. Söbester, A. Keane "Engineering Design via Surrogate Modelling: a practical guide", Chichester, UK, Wiley, 2008.

- [25] I. Couckuyt, T. Dhaene, P. Demeester “ooDACE toolbox, A Matlab Kriging toolbox: Getting started”, 3rd June 2013.
- [26] V. R. Joseph, Y. Hung, A. Sudjianto “Blind Kriging: A New method for Developing Metamodels”, Journal of Mechanical Design, Vol. 130, Issue 3, Research Paper, February 04, 2008.
- [27] I. Couckuyt, A. Forrester, D. Gorissen, F. De Turck, T. Dhaene “Blind Kriging: Implementation and performance analysis”, Advances in Engineering Software, Vol. 49, pp. 1-13, July 2012.
- [28] I. Couckuyt, F. Declercq T. Dhaene, H. Rogier, L. Knockaert “Surrogate-based infill optimization applied to electromagnetic problems”, Special Issue on Advances in Design Optimization of Microwave/RF Circuits and Systems, Vol. 20, No. 5, pp. 492-501, September 2010.
- [29] G. Georgiou, H. H. Khodaparast, J. E. Cooper “Uncertainty Quantification of Aeroelastic Stability”, Mathematics of Uncertainty Modeling in the Analysis of Engineering and Science Problems, IGI Global, 2014, pp.329-356.
- [30] J.D. Martin, T.W. Simpson “On the use of Kriging Models to approximate deterministic computer models”, in Proceedings of DETC’04: ASME 2004 International Design Engineering Technical Conference and Computer and Information in Engineering Conference, Salt Lake City, Utah USA, September 28 – October 2, 2004.
- [31] StatSoft, Inc. (2013). Electronic Statistics Textbook. Tulsa, OK: StatSoft. WEB: <http://www.statsoft.com/textbook/>.
- [32] M.T. Tong, “A Probabilistic Approach to Aeropropulsion System Assessment”, NASA Technical Reports Server NASA/TM-2000-210334, Glenn Research Center, Cleveland, Ohio, USA.